A CFD Model for Synthesis of Dimethyl Ether Directly from Syngas in a Pseudo-Homogeneous Fixed Bed Reactor

Tejbir Singh
Department of Chemical Engineering
National Institute of Technology, Srinagar, India-191006

Abstract

A CFD-model for direct synthesis of Dimethyl Ether (DME) from syngas in a fixed packed bed reactor is presented. One of the recent methods of DME production is the direct conversion of syngas over a dual-catalyst mixture. For the above model, Graaf kinetic model for methanol synthesis and Bercic model for methanol dehydration are used. Three-dimensional CFD simulations of the reactor are demonstrated at operating conditions of 250°C temperature and 8 bar pressure. The compositions of the reactants in the feed streams are 0.32 Carbon-mono-oxide, 0.64 Hydrogen and 0.04 Carbon-dioxide. The simulation results are validated with the available experimental results and further analyzed. The partial pressures of different species are studied in reactor and with respect to time as well, the overall conversion of CO is noted to be 36% in comparison to the experimental value of 38%. The present CFD model results match well with experimental data. The concentration profile of species in terms of partial pressure within the reactor has been analyzed at different fraction of length as well as at different time level. From the results it is concluded that present CFD-model could be a starting point for further studies on the optimization of reactor performance.

Keywords: Direct DME synthesis; CFD Modelling; ANSYS FLUENT; Pseudo-homogeneous porous bed

I. INTRODUCTION

World's energy consumption is to increase by 49% from 2007 to 2035 as predicted by the International Energy Agency. Over this period, the demand of petroleum fuels in the transportation sector is expected to grow by 1.3% annually [1]. Global warming, local emissions, energy security concerns and increasing cost of unconventional oil resources promote the development of processes for production of liquid fuels from natural gas, biomass or coal. DME is ultra-clean, ozone-friendly fuel and already used as aerosol propellant [2]. Its high cetane number and low combustion exhaust emissions turn it into a promising diesel substitute [3, 4] and it is safe in handling [5].

DME is emerging as a future clean fuel. DME diesel fuel provides smokeless combustion, low CO_2 and 90% less NOx emissions than standard automotive fuels [5, 6, 7, 8]. Analyzing many life cycles it is noticed that DME is the most efficient fuel based on renewable feedstock, when the entire chain is taken into account. DME efficiency can be up to five times more than traditional fuels, resulting in less energy wastage and better use of resources. The market for DME has grown globally and significantly during the past few years. Driven by growing demand in Asia-Pacific region the market of DME is to grow very rapidly in next five years [9].

Several works for improving the synthesis of DME form syngas has been done. Recently direct synthesis of DME from syngas has taken attention as it is more efficient than other processes like dehydration of methanol. A single step process is developed by the companies like Haldor Topsoe, JFF Holdings, Korea Gas Corporation, Air Products, NKK [10, 11]. To understand the process and improve the efficiency of the production technology, it is important to identify the effecting parameter. So far Microchannels have been proved to be good as they have better mass and heat transfer than other reactors [12]. Microchannels have high surface to volume ration and a short distance to wall, hence improved heat and mass transfer [11, 12]. Microchannel reactors can be used in identifying the effecting parameter in DME to increase the yield. Microchannel reactors can also be used commercially as they can have the mass production of up to 2500t/d [13]. CFD Models are attracting focus for studying the chemical processes. CFD has been a good tool to study the different parameters like temperature, pressure etc. Through CFD model it has bees showed that the temperature increase in a microchannel reactor for direct DME synthesis is only about 1 °C [12]. The 2-D asymmetric homogeneous porous bed model has also been presented for DME formation from methanol dehydration in an adiabatic reactor [21].

II. PROCEDURES

A. Experimental Data

Experimental data used in this study to validate the model is taken from the work of Hadipour and Sohrabi [14]. A packed bed reactor of 6.4 mm diameter and 650 mm length has been used in the experiment. Table 1 describes the experimental conditions.

B. Reaction Mechanism

Reactions involved in the DME synthesis are as follows:
Methanol synthesis from CO:

$$CO + 2\,H_2 \leftrightarrow C\,H_3OH \qquad -90.4\ kJ/mol \qquad (i)$$

Methanol synthesis from CO2:

$$CO_2 + 3\,H_2 \leftrightarrow C\,H_3OH + H_2O \qquad -49.4\ kJ/mol \qquad (ii)$$

Water gas shift:

$$CO + H_2O \leftrightarrow CO_2 + H_2 \qquad -41.0\ kJ/mol \qquad (iii)$$

Methanol dehydration:

$$2\,CH_3OH \leftrightarrow CH_3OCH_3 + H_2O \qquad -23.0\ kJ/mol \qquad (iv)$$

Several reaction rate kinetic have been derived for the above set of reactions. The combination of methanol formation reaction from Graaf et al. [16, 17, 18] and DME formation from Bercic and Levec [19, 20] are used.

III. MODEL DEVELOPMENT

A 3-D geometry of reactor has been developed using GAMBIT 2.4.6. A packed bed has been developed using FLUENT. On the basis of average catalyst particle diameter and porosity defined in the experimental setup of Hadipour and Sohrabi [14], the user inputs are calculated to develop porous bed using the FLUENT cell zone condition function.

It has been showed that there is no significant change in temperature in a microchannel reactor for direct DME synthesis process [12] and If an exothermic reaction occurring in an adiabatic bed is associated with a mild heat generation, pseudo-homogeneous models are suitable to describe the behaviour of the reactor [15]. Also, the interfacial and inter-particle resistance of mass and heat transfer in catalyst particles can be omitted. Therefore, a pseudo-continuum plug-flow homogeneous reaction model is used to simulate the present model. The model geometry is shown in Fig. 1.

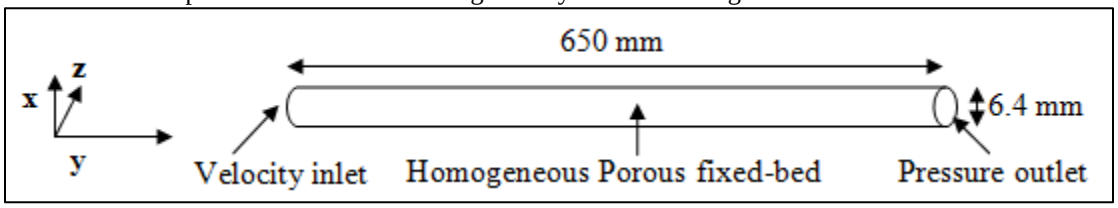

Fig. 1: Diagram of fixed bed reactor.

Table – 1
Experimental data from Hadipour and Sohrabi.[14]

Temperature (°C)	*200-300*
Pressure (barg)	*8*
Velocity (m/s)	*0.163 to 0.033*
CO_x/H_2	*1:2*
Catalyst used	*$CuO/ZnO/ Al_2O_3/\gamma\text{-}Al_2O_3$*
Catalytic bed porosity	*0.32*
Catalyst Particle mean diameter (mm)	*0.104*
Kinetic Model used	*Graaf Model and Bercic Model*

The above model is operated at 250 °C and 8 barg pressure with no slip condition at the reactor wall. The velocity is considered to be 0.0333 m/s at inlet of reactor. The boundary condition of pressure outlet is given at outlet of reactor. A pressure based coupled algorithm is used to solve the governing equations with second order upwind scheme.

C. Governing Equations

The equations solved by FLUENT are as follows.

Continuity Equation

$$\frac{\partial \rho}{\partial t} + \sum_{i=x,y,z} \frac{\partial (\rho\, v_i)}{\partial i} = 0 \qquad (1)$$

$$\frac{\partial \rho v_i}{\partial t} + \left(\sum_{j=x,y,z} \frac{\partial (\rho v_j)}{\partial j} \right) . v_i = \sum_{j=x,y,z} \frac{\tau_{j,i}}{\partial j} - \frac{\partial p}{\partial i} + \rho g_i + \vec{F} \quad (2)$$

Momentum Equations

$$\tau_{i,j} = 2\mu \frac{\partial v_i}{\partial i} - \frac{2}{3}\mu(\nabla . V) \qquad i = j \quad (3)$$

$$\tau_{i,j} = \tau_{i,j} = \mu \left(\frac{\partial v_i}{\partial j} + \frac{\partial v_j}{\partial i} \right) \qquad i \neq j \quad (4)$$

$$F_i = -\left(\frac{150\,(1-\varepsilon)^2 \mu}{D_p^2 \varepsilon^3} v_i + \frac{1.75\,\rho\,(1-\varepsilon)}{D_p \varepsilon^3} |v| v_j \right) \quad (5)$$

Energy Equation

$$\frac{\partial (\rho_k c_{p,k} T_k)}{\partial t} + \left(\sum_{i=x,y,z} \frac{\partial (c_{p,k} v_i T_k)}{\partial i} \right) = \lambda_k \left(\sum_{i=x,y,z} \frac{\partial^2 (T_k)}{\partial i^2} \right) + Q_k R_k \quad (6)$$

Species Transport Equation

$$\frac{\partial (\rho_k Y_k)}{\partial t} + \left(\sum_{i=x,y,z} \frac{\partial (\rho_k v_i Y_k)}{\partial i} \right) = \rho_k D_{k,m} \left(\sum_{i=x,y,z} \frac{\partial^2 (Y_k)}{\partial i^2} \right) + R_k \quad (7)$$

D. Grid Independency Test

The present geometry is tested to give grid independent results. For it, simulations are to be run on same geometry for different grid size, generally taken successively smaller in size. Pressure drop across the porous bed for different velocities and for different grid size is noted and the compared. Grid size of 0.0005 m, 0.0007 m and 0.0009 m are taken to check geometry for giving grid independent results which is shown by solid, dashed and dotted line respectively in Fig. 2.

In Fig. 2, a plot of pressure drop across the porous bed at different velocities for different grid size is shown. There is negligible transition in pressure drop profile across the porous bed while moving from grid size 0.0005 m to 0.0009 m. For present work 0.0005 m grid size is chosen

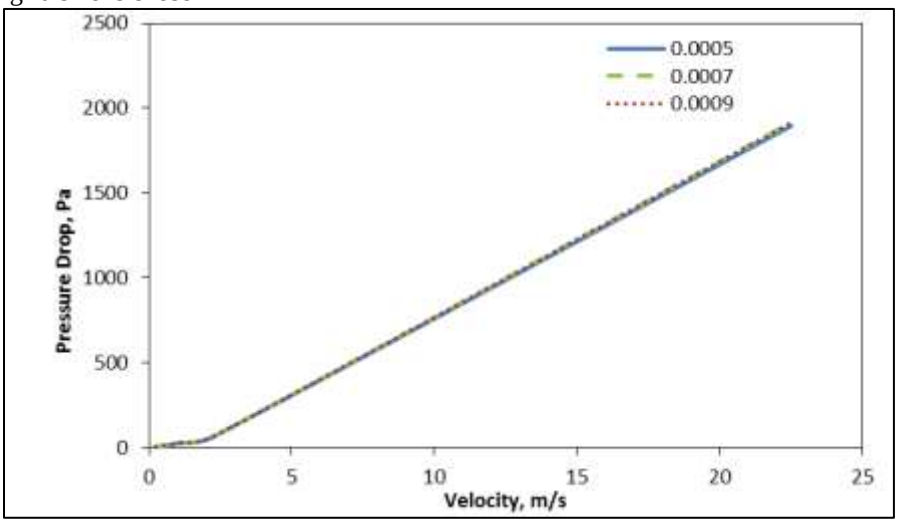

Fig. 2: Plot between velocity and pressure drop across the porous bed for different grid sizes.

E. Validation of flow in porous bed

Flow in the porous bed model is to be verified by using data available in open literature. To analyze the laminar to turbulent transition of flow friction factors are compared. Friction factor can be calculated from equation 8 and 9.

$$f = \frac{64}{\mathrm{Re}} \quad (8)$$

$$\tau_w = \frac{f \rho V^2}{8} \quad (9)$$

In present model friction factor at different Reynolds number is calculated by both equations but using the value of shear stress (τ_w) taken from simulation results in equation 9. These two calculated friction factors are compared in Fig. 3 for flow validation in porous bed. The relative percentage is under 10%. Hence flow in present model is fully laminar for Reynolds number upto 1000.

F. Validation of pressure drop across porous bed using Ergun equation

Ergun (1952) equation is used for calculating friction factor in packed beds. In present work pressure drop taken from simulation results is used to calculate the friction factor and then compared to that is calculated using Reynolds number. By comparing the friction factor from Ergun equation (equation 10) and the value by using pressure drop across the porous bed is validated.
Ergun equation:

$$f_p = \frac{150}{\mathrm{Re}_p} + 1.75 = \frac{\Delta p D_p \varepsilon^3}{L \rho V_s^2 (1-\varepsilon)} \quad (10) \text{ Where, } \mathrm{Re}_p = \frac{D_p \rho V_s}{(1-\varepsilon)\mu} \quad (11)$$

Fig. 4 shows the friction factors comparison and the relative percentage error is less than 5%. Hence the pressure drop across the porous bed is validated with Ergun (1952).

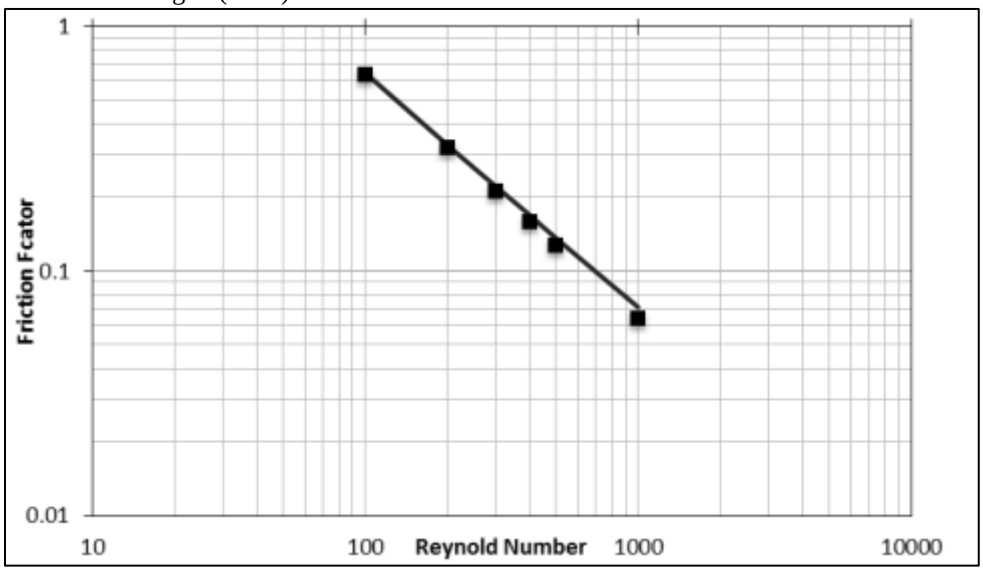

Fig. 3: Comparison of theoretical (dots) and calculated (solid line) friction factors (using shear stress from simulation data) at different Reynolds number.

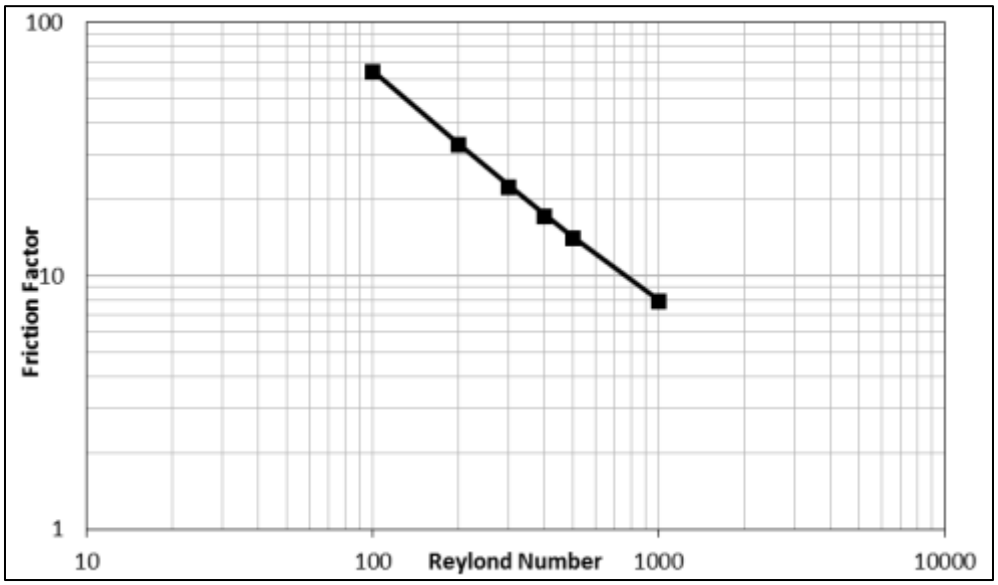

Fig. 4: Comparison of theoretical (dots) and calculated (solid line) friction factors (using pressure drop from simulation data) at different Reynolds number.

IV. RESULTS AND DISCUSSION

A. Validation of model

The present model is simulated transiently for the reactions (i) to (iv) with time step of one second. The partial pressures of different species are observed over the time period of 480 minutes.

Fig. 5, Fig. 6 and Fig.7 show the partial pressure of methanol, partial pressure of DME and conversion of CO at reactor outlet respectively. Initially the simulated results are shattered, the apartness observed in the initial time period is due to time taken by FLUENT solver to set the flow across the channel. Or it may be due to predicting an unsteady state model results with steady state experimental results. There is a peak in Fig. 5 which shows that the overall reaction is series reaction in which methanol is acting as an intermediate. The overall reaction of DME synthesis follows the reaction in series mechanism in which methanol act as the intermediate species hence the nature of curve is increasing initially as shown in Fig.5. The outlet concentration in terms of partial pressure and the overall conversion is well in the acceptable range as can be seen from Fig. 5, Fig 6 and Fig. 7.

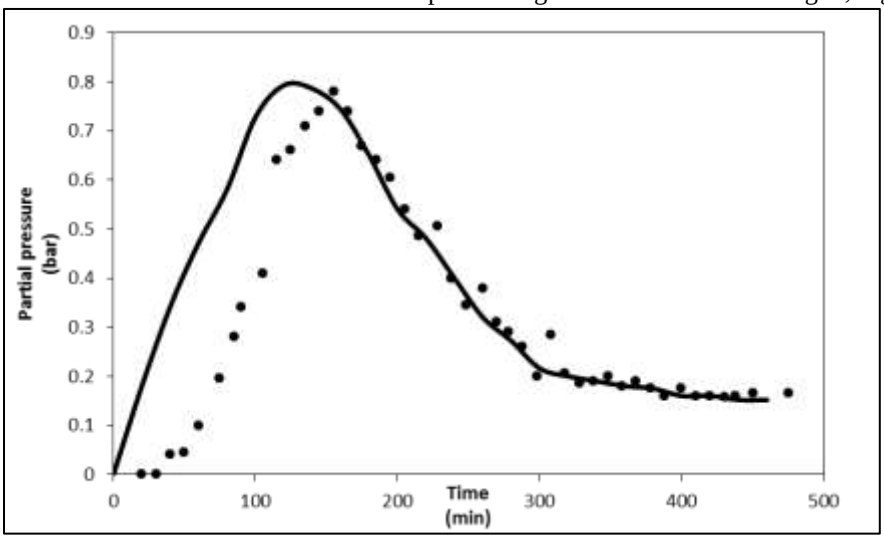

Fig. 5: Graphical representation of simulation (solid line) and experimental (dots) data [Hadipour] of partial pressure of methanol at reactor outlet.

B. Concentration profile of species at different length

Fig. 8 to Fig. 10 shows the partial pressure of methanol, partial pressure of DME and the conversion of CO at different fraction of length of the reactor respectively. The partial pressure of species and conversion of CO is increasing with the reactor length.

Fig. 11 and Fig. 12 shows the methanol partial pressures for different time with respect to length of reactor obtained from simulation results. There is increment and decrement in the methanol partial pressure at outlet on each side of maxima. Similarly Fig. 13 and Fig. 14 shows the partial pressure and conversion of CO at different time, here also the partial pressure and conversion is increasing with time which eventually reached to the steady state.

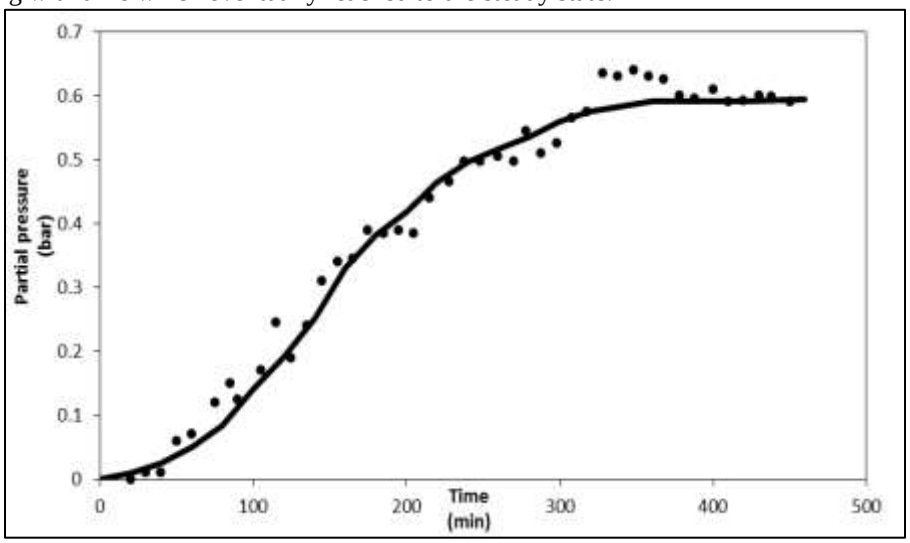

Fig. 6: Graphical representation of simulation (solid line) and experimental (dots) data (Hadipour) of partial pressure of dimethyl ether at reactor outlet.

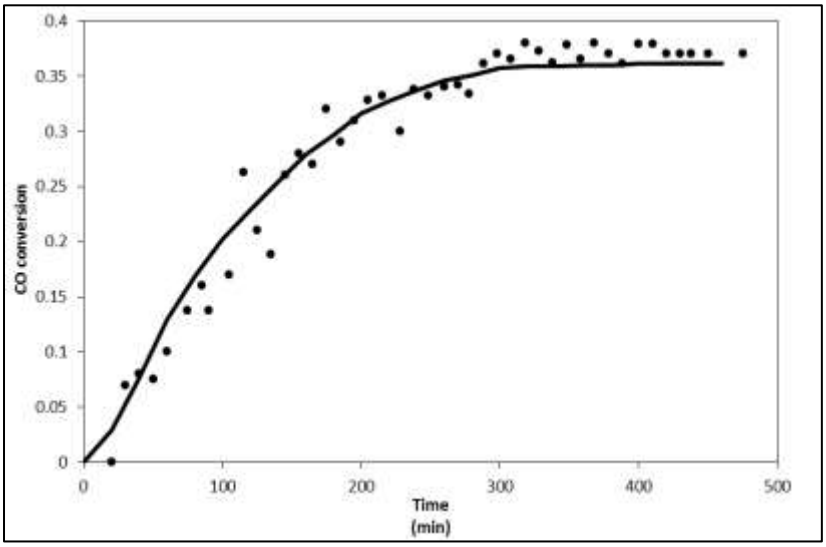

Fig. 7: Graphical representation of simulation (solid line) and experimental (dots) data (Hadipour) of conversion of carbon mono oxide at reactor outlet

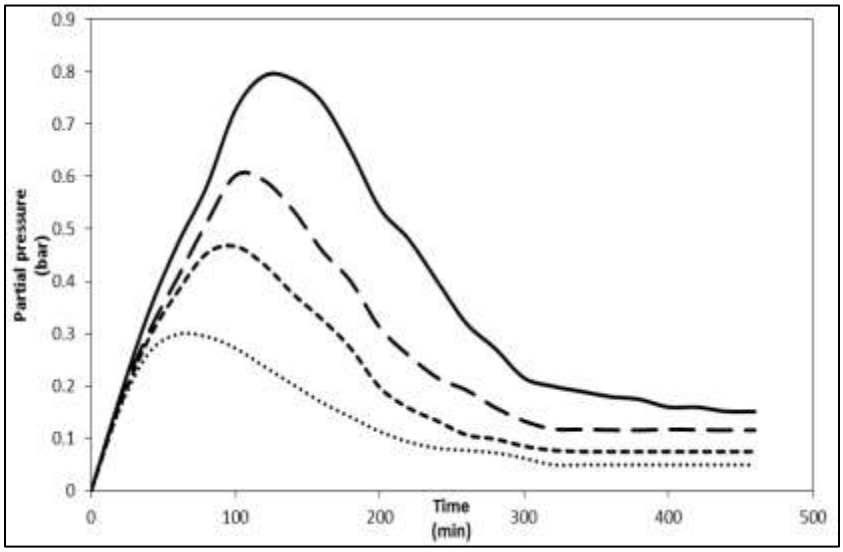

Fig. 8: Graphical representation of partial pressure of methanol for different fraction of reactor length. Z=L (solid line), Z=3L/4 (Long dash line), Z=L/2 (dashed line), Z=L/4 (dotted line).

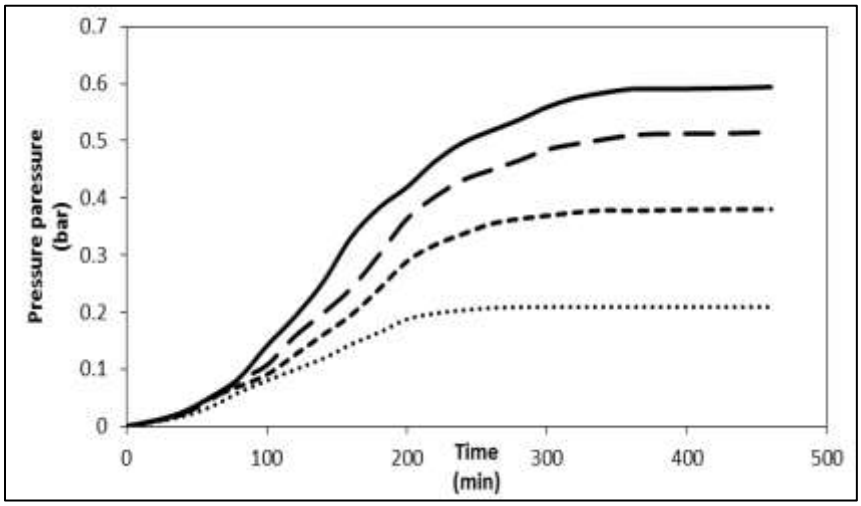

Fig. 9: Graphical representation of partial pressure of DME for different fraction of reactor length. Z=L (solid line), Z=3L/4 (Long dash line), Z=L/2 (dashed line), Z=L/4 (dotted line).

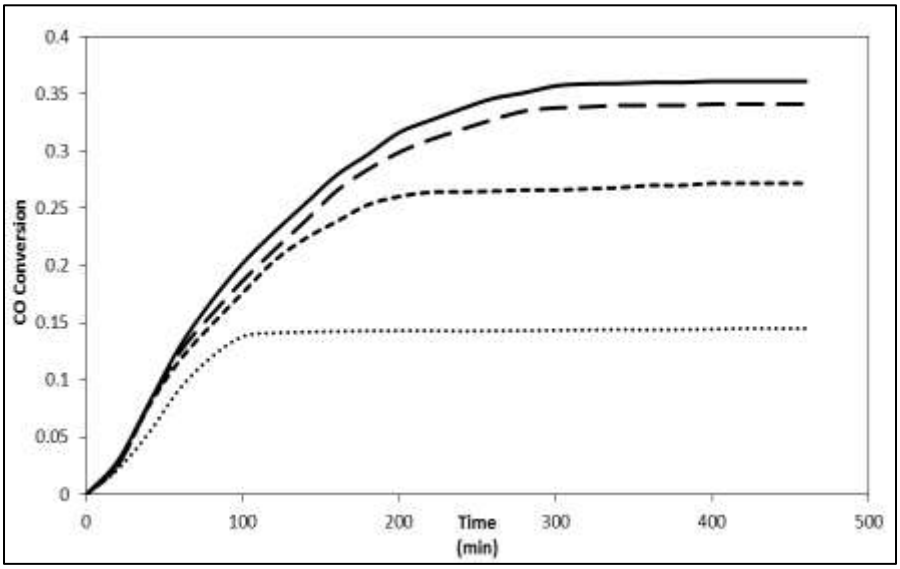

Fig. 10: Graphical representation of conversion of CO for different fraction of reactor length. Z=L (solid line), Z=3L/4 (Long dash line), Z=L/2 (dashed line), Z=L/4 (dotted line).

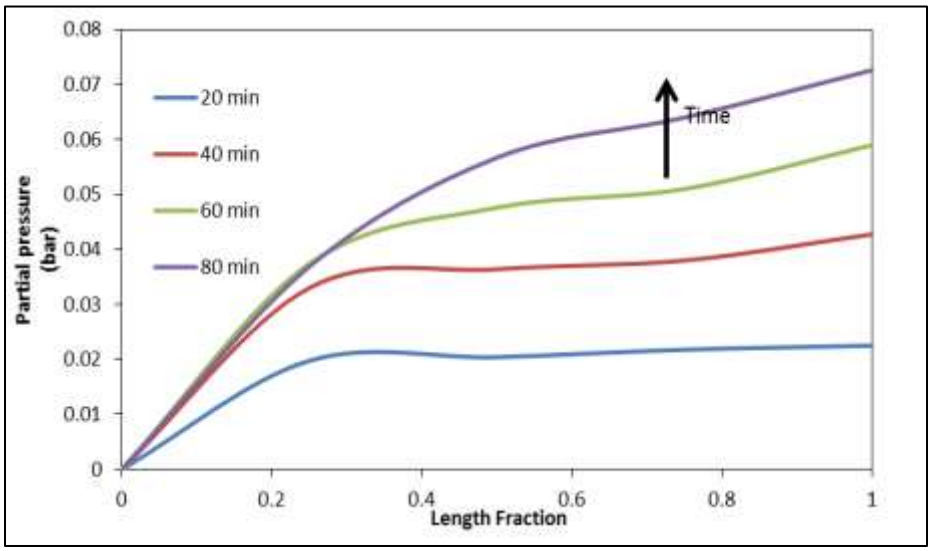

Fig. 11: Graphical representation of partial pressures of methanol for different time with respect to length of reactor before maximum point.

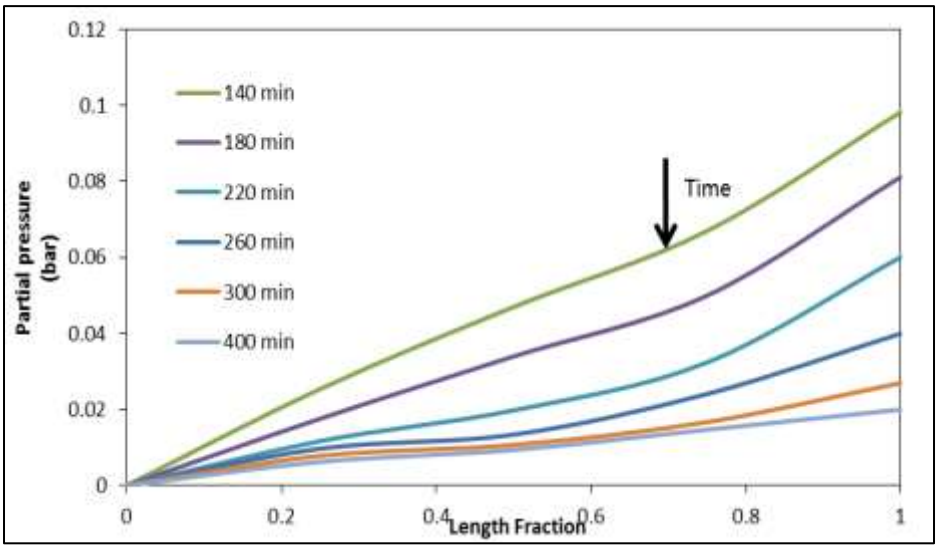

Fig. 12: Graphical representation of partial pressures of methanol for different time with respect to length of reactor after maximum point.

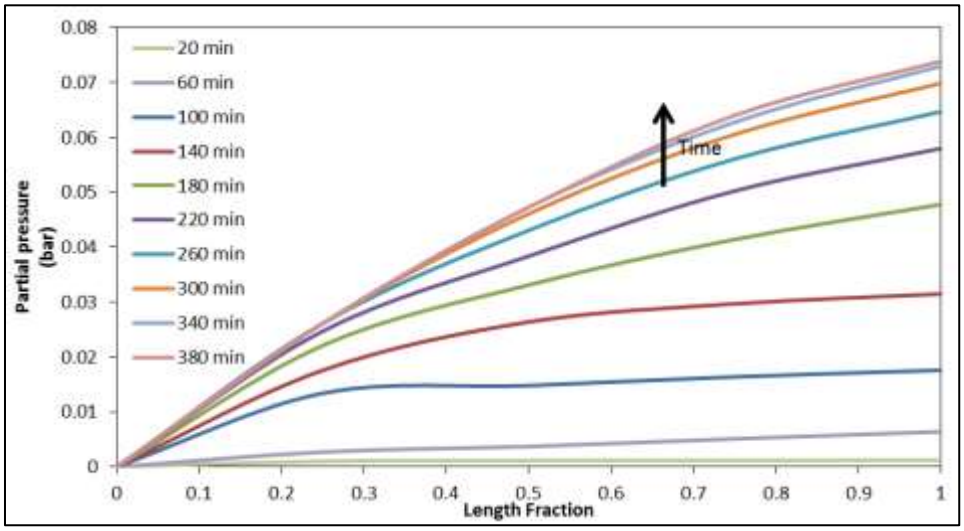

Fig. 13: Graphical representation of partial pressures of dimethyl ether for different time with respect to length of reactor.

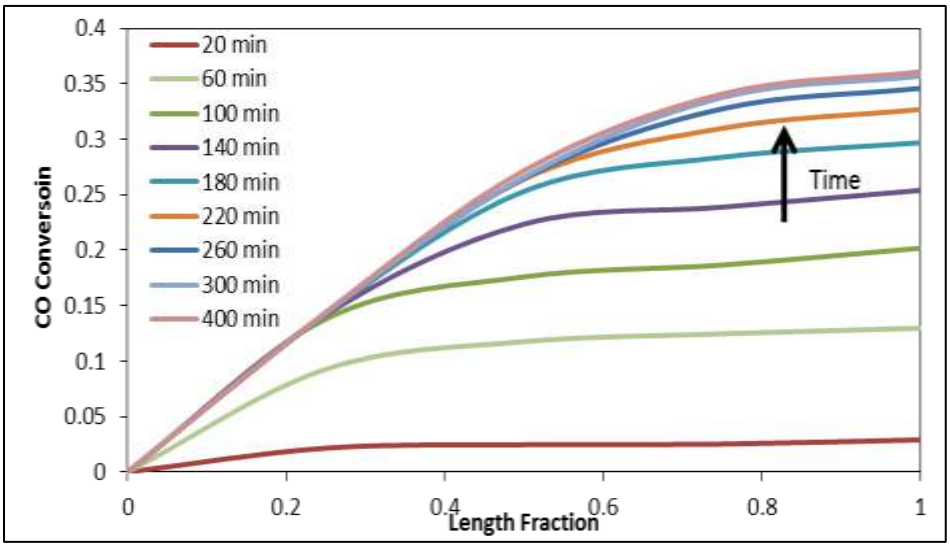

Fig. 14: Graphical representation of conversion of CO for different time with respect to length of reactor.

It is clearly proved that the present model is the replica of the experimental setup and can be used for prediction of any data by simulating the model for particular set of operating conditions hence saving the experimental material and time.

V. CONCLUSION

A two-dimensional homogenous fixed bed is modelled in FLUENT 14.5 is validated by the experimental data. The present study discusses partial pressure of CO, Methanol, DME at the reactor outlet. The model also predicts the friction factor within an error of 0.96 % relative to calculated using the Ergun equation. The combination of Graaf Model for methanol synthesis and Bercic Model for methanol dehydration are used in the present work. The simulations were carried out at the temperature of 250 °C and pressure of 8 bars. The partial pressures at the reactor outlet are obtained and it has been shown that the error is less than 10 % with the experimental data. The partial pressures in the reactor were analysed with respect to time and length as well. It is concluded that a pseudo homogeneous model in FLUENT can be used to predicts the results.

NOMENCLATURE

c_i Concentration i-componenet (kgmol)
$c_{p,k}$ Specific heat of k-species (KJ/kg.K)
D_k Mass diffusion of k-species in mixture (m^2/s)
D_p Particle diameter (m)
f Friction factor
L Length of reactor (m)

p Pressure (Pa)
Q Heat of reaction (KJ/kmol)
T Temperature (K)
t Time (s)
v_i Velocity in i-direction (m/s)
Y_k Mole fraction

GREEK SYMBOL

ε Porosity of packed bed
μ Viscosity (kg/m.s)
ρ Density (kg/m^3)

SUBSCRIPTS

i x, y, z
j x, y, z
k CO, H_2 , CO_2 , CH_3OH, H_2O, CH_3OCH_3

REFERENCES

[1] International Energy Outlook, US EIA (2010).
[2] C.W. Simons, J. O'Neill, J.A. Gribens, US Patent 4,041,148 (1977)
[3] F. Maroteaux, G. Descombes, F. Sauton, J. Jullien, International Journal of Engine Research 2, 199–207 (2001)
[4] Arcoumanis, C. Bae, R. Crookes, E. Kinoshita, Fuel 87, 1014–1030 (2008)
[5] F. Raoof, M. Taghizadeh, A. Eliassi, F. Yaripour, Fuel 87, 2967–2971 (2008)
[6] K.C. Tokay, T. Dogu, G. Dogu, Chem. Eng. J. 184, 278 (2012)
[7] W.-H. Chen, B.-J. Lin, H.-M. Lee, M.-H. Huang, Appl. Energy 98, 92–101(2012)
[8] F. Hayer, H. Bakhtiary-Davijany, R. Myrstad, A. Holmen, P. Pfeifer, H.J. Venvik, Chem. Eng. Process. 70, 77–85 (2013)
[9] DME Association
[10] M. G, adek, R. Kubica, E. J, edrysik, The 23rd European Symposiumon Computer Aided Process Engineering (ESCAPE 23), 9–12 (2013)
[11] E. Ren, J.-F. Wang, H.S. Li, Stud. Surf. Sci. Catal.159, 489–492 (2006)
[12] F. Hayer, H. Bakhtiary-Davijany, R. Myrstad, A. Holmen, P. Pfeifer, H.J.Venvik, Chem. Eng. J. 167, 610 (2011)
[13] Y. Adachi, M. Komoto, I. Watanabe, Y. Ohno, K. Fujimoto, Fuel 79, 229–234 (2000)
[14] Ali Hadipour and Morteza Sohrabi, J. Ind. Eng. Chem. 13, 558-565 (2007)
[15] Andrigo, P., Bagatin, R. and Pagani, G., Catalysis Today 52, 197-221(1999)
[16] G. H. Graaf, J. G. M. Winkelman, E. J. Stamhuis, and A. A. C. M. Beenakers, Chem. Eng. Sci. 43, 2161-2168 (1988)
[17] G. H. Graaf, P. J. J. M. Sijtsema, E. J. Stamhuis, and G. E. H. Joosten, Chem. Eng. Sci. 41, 2883-2890 (1986).
[18] G. H. Graaf E. J. Stamhuis, and A. A. C. M. Beenakers, Chem. Eng. Sci. 43, 3185-3195 (1988).
[19] G. Bercic and J. Levec, Ind. Eng. Chem. Res. 31, 1035 (1992).
[20] G. Bercic and J. Levec, Ind. Eng Chem. Res. 32, 2478 (1993).
[21] M. Golshadi, R. Mosayebi Behbahani, and M. Irani, Iranian Journal of Oil & Gas Science and Technology 2, 50-64 (2013)